

Recent experimental results on charmed baryons

M. J. Charles*¹

¹University of Oxford, Oxford, OX1 3RH, UK

Introduction

This paper summarizes recent experimental results on charmed baryons, as presented at the Third International Workshop on Charm Physics, 20–22 May 2009, Heidelberg, Germany [1]. Two main topics are covered: first, the spectroscopy of charmed baryon states; second, the production of charmed baryons in the decays of B mesons and from the e^+e^- continuum.

Spectroscopy

There has been a steady progression of results on charmed baryon spectroscopy from the e^+e^- B -factories BABAR [4] and Belle [5] in recent years, building on the foundations laid by CLEO, FOCUS, E687, ARGUS, and others [6]. We summarize new and interesting results for Σ_c , Ξ_c , and then Ω_c states.

Σ_c states

BABAR has recently published a study of the decay $B^- \rightarrow \Lambda_c^+ \bar{p} \pi^-$ in a sample of $383 \times 10^6 \Upsilon(4S) \rightarrow B\bar{B}$ decays [7, 3] measuring $\mathcal{B}(B^- \rightarrow \Lambda_c^+ \bar{p} \pi^-) = (3.38 \pm 0.12 \pm 0.12 \pm 0.88) \times 10^{-4}$ [2]. This value is somewhat larger than the previous Belle result of $(2.01 \pm 0.15 \pm 0.20 \pm 0.52) \times 10^{-4}$ from $152 \times 10^6 \Upsilon(4S) \rightarrow B\bar{B}$ decays [8]. Both papers see clear signals for $B^- \rightarrow \Sigma_c(2455)^0 \bar{p}$ in the Dalitz plot, but a small or no signal for $B^- \rightarrow \Sigma_c(2520)^0 \bar{p}$. Both papers also observed a $\Lambda_c^+ \bar{p}$ threshold enhancement, discussed later. In addition, BABAR noted a broad, statistically significant (5.8σ) peak in $\Lambda_c^+ \pi^-$ which is well-described by a relativistic D -wave Breit-Wigner with mass $2846 \pm 8 \text{ MeV}/c^2$ and width $86_{-22}^{+33} \text{ MeV}$, as illustrated in Fig. 1. This region of the Dalitz plot is populated in the Belle data, but it is not clear whether a significant structure with the same parameters is present. The closest known resonance is the $\Sigma_c(2800)^0$ [9]: the widths are consistent but the mass obtained by BABAR differs from the nominal value, $2802 \pm 4 \pm 7 \text{ MeV}/c^2$, by around three standard deviations. This difference is intriguing but not conclusive. An updated study by Belle with their large $\Upsilon(4S)$ dataset could settle this question and establish whether BABAR saw the $\Sigma_c(2800)^0$ with a downward fluctuation in mass or an entirely new state.

BABAR also used the large $B^- \rightarrow \Sigma_c(2455)^0 \bar{p}$ signal to determine the spin of the $\Sigma_c(2455)^0$; the state is predicted to have $J^P = 1/2^+$ in the quark model but neither quantum number has been measured. BABAR performed an angular analysis of the decay under the assumption that $J(\Lambda_c^+) =$

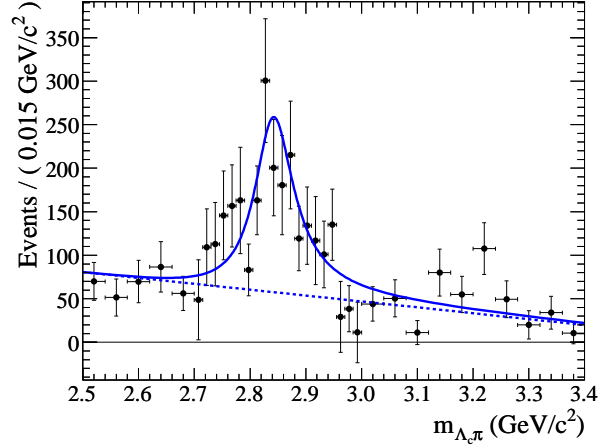


Figure 1: The $m(\Lambda_c^+ \pi^-)$ invariant mass distribution from $B^- \rightarrow \Lambda_c^+ \bar{p} \pi^-$ data at BABAR, using a likelihood weighting technique to suppress background. From [7].

$1/2$, testing the data for consistency with a spin of $1/2$ or $3/2$ for the $\Sigma_c(2455)^0$. Defining the helicity angle θ_h as the angle between the momentum vector of the Λ_c^+ and the momentum vector of the recoiling B -daughter \bar{p} in the rest frame of the $\Sigma_c(2455)^0$, the expected angular distributions are:

$$J(\Sigma_c(2455)^0) = 1/2 : \frac{dN}{d \cos \theta_h} \propto 1$$

$$J(\Sigma_c(2455)^0) = 3/2 : \frac{dN}{d \cos \theta_h} \propto 1 + 3 \cos^2 \theta_h.$$

The measured helicity angle distribution, shown in Fig. 2, is found to be consistent with spin- $1/2$ but inconsistent with spin- $3/2$ by more than four standard deviations.

Ξ_c states

There has been a flurry of results on new Ξ_c states in the past three years, beginning with the first observations of the $\Xi_c(2980)$ and $\Xi_c(3077)$ isodoublets by Belle in the $\Lambda_c^+ K^- \pi^+$ and $\Lambda_c^0 \bar{K}^0 \pi^+$ final states with 462 fb^{-1} of data [10]. These were subsequently confirmed by BABAR [11], who also reported two other possible structures, denoted $\Xi_c(3055)^+$ and $\Xi_c(3123)^+$, in 384 fb^{-1} of data. Belle has also observed the $\Xi_c(2980)$ in the final states $\Xi_c(2645)^0 \pi^+$ and $\Xi_c(2645)^+ \pi^-$ in a separate study of 414 fb^{-1} of data [12]. The current understanding of these states is summarized below. The resonance parameters are given in Table 1.

The $\Xi_c(2980)$ resonances are now well-established, having been seen with large significance in more than one final

* m.charles1@physics.ox.ac.uk

Table 1: Results on new Ξ_c resonances. The mass, width, and (where given) statistical significance are listed.

Source	Resonance and final state	Mass (MeV/ c^2)	Width (MeV)	Signif.
BABAR [13]	$\Xi_c(2930)^0 \rightarrow \Lambda_c^+ K^-$	$2931 \pm 3 \pm 5$	$36 \pm 7 \pm 1$	
Belle [10]	$\Xi_c(2980)^+ \rightarrow \Lambda_c^+ K^- \pi^+$	$2978.5 \pm 2.1 \pm 2.0$	$43.5 \pm 7.5 \pm 7.0$	6.3σ
BABAR [11]	$\Xi_c(2980)^+ \rightarrow \Lambda_c^+ K^- \pi^+$	$2969.3 \pm 2.2 \pm 1.7$	$27 \pm 8 \pm 2$	$> 9.0\sigma$
Belle [12]	$\Xi_c(2980)^+ \rightarrow \Xi_c(2645)^0 \pi^+$	$2967.7 \pm 2.3^{+1.1}_{-1.2}$	$18 \pm 6 \pm 3$	7.3σ
Belle [10]	$\Xi_c(2980)^0 \rightarrow \Lambda_c^+ \bar{K}^0 \pi^-$	$2977.1 \pm 8.8 \pm 3.5$	43.5 (fixed)	2.0σ
BABAR [11]	$\Xi_c(2980)^0 \rightarrow \Lambda_c^+ \bar{K}^0 \pi^-$	$2972.9 \pm 4.4 \pm 1.6$	$31 \pm 7 \pm 8$	1.7σ
Belle [12]	$\Xi_c(2980)^0 \rightarrow \Xi_c(2645)^+ \pi^-$	$2965.7 \pm 2.4^{+1.1}_{-1.2}$	$15 \pm 6 \pm 3$	6.1σ
BABAR [11]	$\Xi_c(3055)^+ \rightarrow \Sigma_c(2455)^+ K^-$	$3054.2 \pm 1.2 \pm 0.5$	$17 \pm 6 \pm 11$	6.4σ
Belle [10]	$\Xi_c(3077)^+ \rightarrow \Lambda_c^+ K^- \pi^+$	$3076.7 \pm 0.9 \pm 0.5$	$6.2 \pm 1.2 \pm 0.8$	9.7σ
BABAR [11]	$\Xi_c(3077)^+ \rightarrow \Lambda_c^+ K^- \pi^+$	$3077.0 \pm 0.4 \pm 0.2$	$5.5 \pm 1.3 \pm 0.6$	$> 9.0\sigma$
Belle [10]	$\Xi_c(3077)^0 \rightarrow \Lambda_c^+ \bar{K}^0 \pi^-$	$3082.8 \pm 1.8 \pm 1.5$	$5.2 \pm 3.1 \pm 1.8$	5.1σ
BABAR [11]	$\Xi_c(3077)^0 \rightarrow \Lambda_c^+ \bar{K}^0 \pi^-$	$3079.3 \pm 1.1 \pm 0.2$	$5.9 \pm 2.3 \pm 1.5$	4.5σ
BABAR [11]	$\Xi_c(3123)^+ \rightarrow \Sigma_c(2520)^+ K^-$	$3122.9 \pm 1.3 \pm 0.3$	$4.4 \pm 3.4 \pm 1.7$	3.0σ

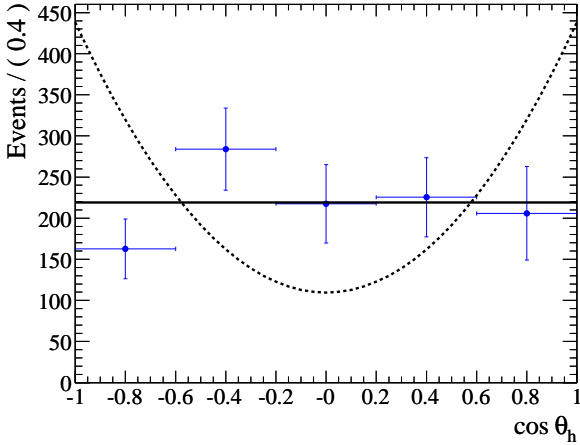


Figure 2: The helicity angle distribution for $\Sigma_c(2455)^0$ candidates in $B \rightarrow \Lambda_c^+ \bar{p} \pi^-$ data at BABAR. From [7].

state. In the discovery mode, $\Lambda_c^+ \bar{K} \pi$, the state is close to the kinematic threshold of $2920 \text{ MeV}/c^2$ —and as noted by BABAR, approximately half of the $\Lambda_c^+ \bar{K} \pi$ decays proceed via an intermediate $\Sigma_c(2455)$, for which the threshold is at $2950 \text{ MeV}/c^2$. The fit is therefore sensitive to the details of the assumptions made about the signal lineshape, the fraction of decays proceeding via a $\Sigma_c(2455)$, and the behaviour of the background near threshold; this led to mildly inconsistent results for the mass and width from Belle and BABAR. The final state $\Xi_c(2645)\pi$, reported by Belle and shown in Fig. 3, is well above threshold and does not suffer from these complications; it also has a much lower background rate and does not require reconstruction of a K_S for either isospin partner.

The narrow $\Xi_c(3077)$ resonances are also well-established: both isospin states have been seen clearly by Belle and BABAR, and there is good agreement about the masses and widths. BABAR has shown that most (if not all) of the decay proceeds via the quasi-two-body processes

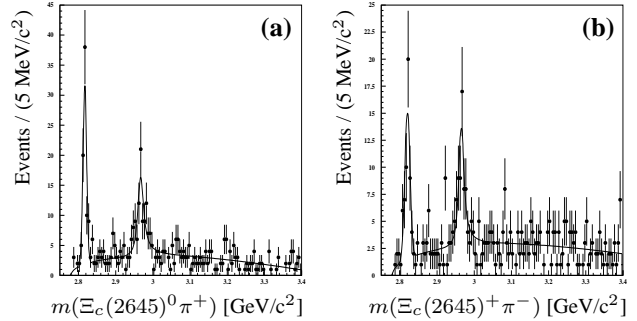


Figure 3: Invariant mass distributions for (a) $\Xi_c(2645)^0 \pi^+$, and (b) $\Xi_c(2645)^+ \pi^-$. The $\Xi_c(2815)$ and $\Xi_c(2980)$ isodoublets are visible. From [12].

$\Xi_c(3077) \rightarrow \Sigma_c(2455)\pi$ and $\Xi_c(3077) \rightarrow \Sigma_c(2520)\pi$ with roughly equal branching fractions.

The $\Xi_c(3055)^+$ and $\Xi_c(3123)^+$ structures have been reported by BABAR in the $\Lambda_c^+ K^- \pi^+$ final state only with statistical significances of 6.4 and 3.0 standard deviations, respectively; they have not yet been confirmed by Belle. The structures are not visible above background in the inclusive $\Lambda_c^+ K^- \pi^-$ mass spectrum but emerge when requiring that the $\Lambda_c^+ \pi^-$ invariant mass lie in a narrow window around the $\Sigma_c(2455)^0$ (for the $\Xi_c(3055)^+$) or the $\Sigma_c(2520)^0$ (for the $\Xi_c(3123)^+$).

BABAR has also searched the inclusive $\Lambda_c^+ \bar{K}$ and $\Lambda_c^+ \bar{K} \pi^+ \pi^-$ invariant mass spectra for evidence of further narrow Ξ_c states but did not find any significant structure above the background.

There is one other candidate for a new Ξ_c state, seen by BABAR in an analysis of $B^- \rightarrow \Lambda_c^+ \bar{\Lambda}_c^- K^-$ in a sample of $230 \times 10^6 \Upsilon(4S) \rightarrow B\bar{B}$ decays [13]. The Dalitz plot, shown in Fig. 4, is clearly inconsistent with a phase-space distribution and is consistent with a dominant contribution from a single Ξ_c^0 resonance with mass $2931 \pm 3 \pm 5 \text{ MeV}/c^2$ and width $36 \pm 7 \pm 1 \text{ MeV}$. However, this structure has not yet been confirmed by Belle. The B decay mode it-

self was first observed by Belle in a sample of 386×10^6 $\Upsilon(4S) \rightarrow B\bar{B}$ decays [14]; the publication included the $\Lambda_c^+\bar{\Lambda}_c^-$ invariant mass spectrum as part of a search for charmonium states but not the full Dalitz plot or the $\Lambda_c^+K^-$ projection.

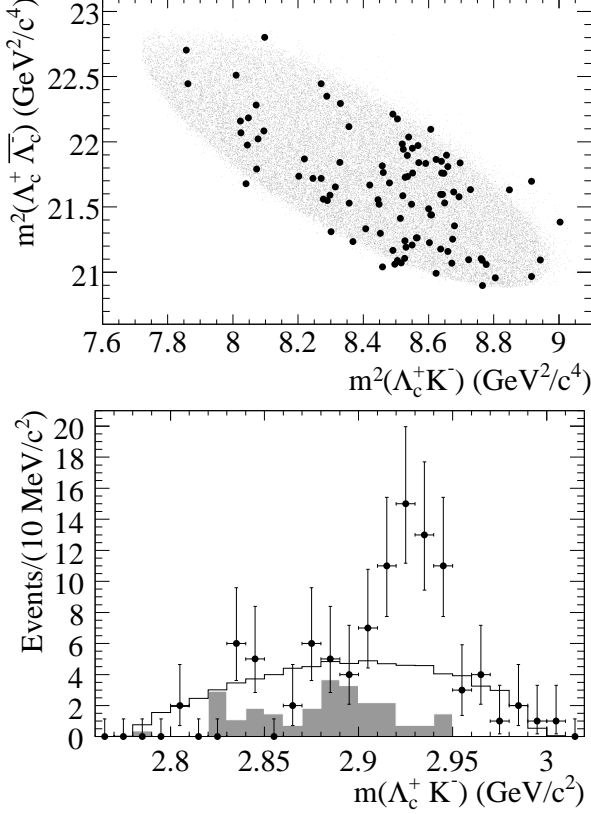


Figure 4: Reconstructed $B^- \rightarrow \Lambda_c^+ \bar{\Lambda}_c^- K^-$ candidates, showing a Dalitz plot (upper) and the $\Lambda_c^+ K^-$ invariant mass distribution (lower). Data from the signal region are shown as black points; signal from a phase-space simulation are shown as small grey points in (a) and as a histogram in (b); and data from a mass sideband region are shown as a shaded histogram in (b), normalized to the expected background in the signal region. From [13].

Ω_c states

The weakly-decaying Ω_c^0 ground state has been established for more than a decade [6], but until recently its properties had only been measured with a handful of events. Both BABAR and Belle have now published studies with large statistics, confirming and expanding upon previous results. BABAR has reported the first observation of Ω_c^0 production in B meson decays with an inclusive method, as shown in Fig. 5, along with measurements of ratios of branching fractions with much improved precision in 231 fb^{-1} of data [15]. In addition, Belle has made a new measurement of the Ω_c^0 mass with 673 fb^{-1} of data [16], obtaining $m(\Omega_c^0) = 2693.6 \pm 0.3^{+1.8}_{-1.5} \text{ MeV}/c^2$.

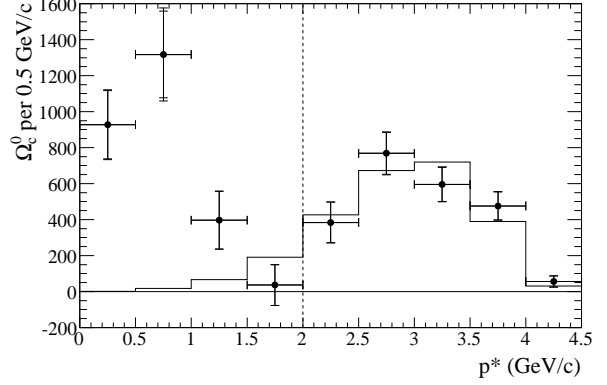


Figure 5: The inclusive momentum spectrum of Ω_c^0 baryons in e^+e^- data at $\sqrt{s} \approx 10.6 \text{ GeV}/c$. The data show two peaks: the one at higher momentum is due to Ω_c^0 production in continuum events, and the one at lower momentum is due to the decays of B mesons. The histogram shows the Bowler fragmentation function, fit to the data above $2 \text{ GeV}/c$. From [15].

The quark model predicts two Ω_c^0 ground states: a lower-mass octet state with $J^P = 1/2^+$ and a higher-mass decuplet state with $J^P = 3/2^+$. This higher-mass partner was observed by BABAR[17] and confirmed by Belle [16] (Fig. 6); this completes the experimental discoveries of all $C = 1$ ground states predicted by the quark model. The mass splitting between the two Ω_c partner states ΔM is measured to be:

$$\begin{aligned} \text{BABAR: } \Delta M &= 70.8 \pm 1.0 \pm 1.1 \text{ MeV}/c^2 \\ \text{Belle: } \Delta M &= 70.7 \pm 0.9^{+0.1}_{-0.9} \text{ MeV}/c^2, \end{aligned}$$

with excellent agreement between the two experiments. Since ΔM is less than the pion mass, there is no allowed strong decay for the heavier partner state and it therefore decays electromagnetically to $\Omega_c^0 \gamma$.

From the constituent quark model [18], we would expect other octet-decuplet mass splittings, $m(\Xi_c(2645)) - m(\Xi_c')$ and $m(\Sigma_c(2520)) - m(\Sigma_c(2455))$, to be comparable to the Ω_c splitting but with some variation due to broken $SU(3)$ symmetry entering via the spin-spin coupling term. It is interesting just how small the variation is; averaging over the isospin states and assuming the uncertainties to be systematics-dominated, the current data give: [6]

$$\begin{aligned} m(\Xi_c(2645)) - m(\Xi_c') &\approx 69.5 \pm 3 \text{ MeV}/c^2 \\ m(\Sigma_c(2520)) - m(\Sigma_c(2455)) &\approx 64.3 \pm 0.5 \text{ MeV}/c^2. \end{aligned}$$

Production of charmed baryons

The production of baryons in e^+e^- interactions and meson decay is still a subject of active study. Charmed baryons provide an excellent laboratory for probing baryon formation, especially at the e^+e^- B -factories where they are produced copiously.

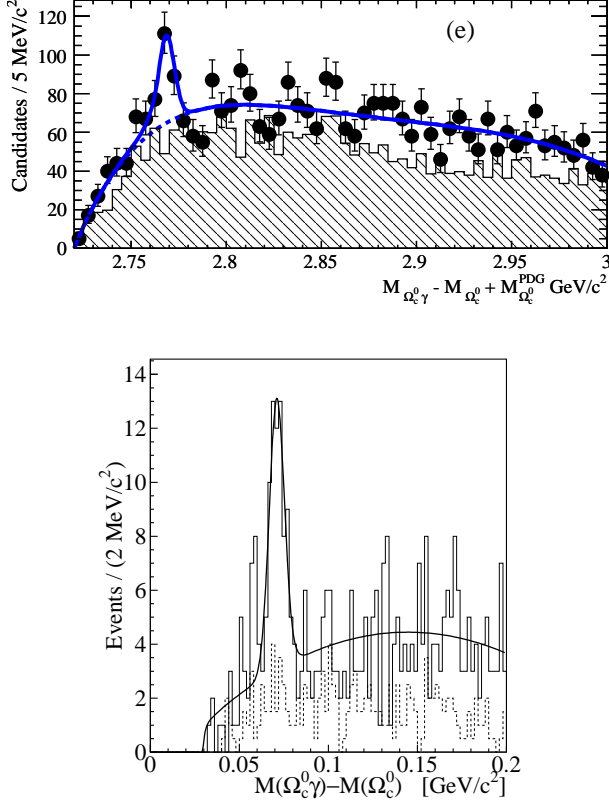


Figure 6: Invariant mass spectra of $\Omega_c \gamma$ at BABAR in 231 fb^{-1} (upper) and Belle in 673 fb^{-1} of data (lower). The $\Omega_c(2770)^0$ resonance is visible in each plot. From [17] and [16].

Two-body B decays to baryons

It has been known for many years that B mesons decay to baryons at a significant rate, with a branching fraction of approximately 7% [19]. However, individual decay modes—especially two-body and quasi-two-body modes—have been challenging to observe. The reason for this is two-fold. First, the branching fractions are often (but not always) small, e.g. $\mathcal{B}(\overline{B}^0 \rightarrow \Lambda_c^+ \overline{p}) = (2.0 \pm 0.4) \times 10^{-5}$, and $\mathcal{B}(\overline{B}^0 \rightarrow p \overline{p}) < 1.1 \times 10^{-7}$ at the 90% confidence limit [6]. Second, non-CKM-suppressed decays involve a charmed particle which must be reconstructed, implying another factor of $\mathcal{O}(\text{few}\%)$ in the yield due to the charm branching fraction.

One notable exception to the first point is $B^- \rightarrow \Xi_c^0 \overline{\Lambda}_c^-$, which was observed by Belle in an analysis of $386 \times 10^6 \Upsilon(4S) \rightarrow B\overline{B}$ decays [20] (along with evidence for its isospin partner mode $B^- \rightarrow \Xi_c^0 \overline{\Lambda}_c^-$) and confirmed by BABAR with a sample of $230 \times 10^6 \Upsilon(4S) \rightarrow B\overline{B}$ decays [13]. They obtained the following values for $\mathcal{B}(B^- \rightarrow \Xi_c^0 \overline{\Lambda}_c^-) \times \mathcal{B}(\Xi_c^0 \rightarrow \Xi^- \pi^+)$:

$$\begin{aligned} \text{Belle:} & \quad (4.8_{-0.9}^{+1.0} \pm 0.9 \pm 1.0) \times 10^{-5} \\ \text{BABAR:} & \quad (2.1 \pm 0.7 \pm 0.3 \pm 0.5) \times 10^{-5}. \end{aligned}$$

The value of $\mathcal{B}(\Xi_c^0 \rightarrow \Xi^- \pi^+)$ has not been measured

experimentally but is expected to be of order 1–2% [21], which would imply $\mathcal{B}(B^- \rightarrow \Xi_c^0 \overline{\Lambda}_c^-) \sim 1 \times 10^{-3}$. This is large compared to other two-body baryonic decay modes, although still smaller than corresponding mesonic decay modes (e.g. $\mathcal{B}(B^- \rightarrow D_s^- D^0) = (1.0 \pm 0.2)\%$ [6]).

Threshold enhancements in B decays to baryons

One explanation for this pattern is that producing a baryon-antibaryon pair with large energy release (i.e. where the baryon and antibaryon have large relative velocity) is kinematically suppressed, since such a reaction requires two hard gluons [22, 23]. This turns the usual intuition on its head: processes with a larger phase space have smaller rates. A corollary is that for three-body (or, in general, multi-body) baryonic B decays with a large energy release, the bulk of the Dalitz plane is kinematically suppressed—but not the region close to the baryon-antibaryon threshold. This implies a kinematic enhancement near the threshold.

Threshold peaks have been seen in a number of baryonic B decays (some illustrated in Fig. 7) including $B^- \rightarrow \Lambda_c^+ \overline{p} \pi^-$, $B^- \rightarrow p \overline{p} \pi^-$, $B^- \rightarrow p \overline{p} K^-$, $B^- \rightarrow \Lambda \overline{\Lambda} K^-$, $B^- \rightarrow \Lambda \overline{p} \gamma$, and $B^0 \rightarrow p \overline{\Lambda} \pi^-$ [7, 24, 25, 26], as well as in other decays such as $J/\psi \rightarrow p \overline{\Lambda} K^-$ and $J/\psi \rightarrow p \overline{p} \gamma$ [27, 28], so there does appear to be a general pattern. However, there are other mechanisms which can also cause a threshold peak—most obviously a resonance at or just below the threshold, but also other effects such as final-state interactions [29, 30, 31]—so the nature of the structure in a particular mode may be more complicated than this. There are also modes where no threshold peak is seen even though it might be expected, e.g. $\overline{B}^0 \rightarrow \Sigma_c(2455)^{++} \overline{p} \pi^-$ and $\overline{B}^0 \rightarrow \Sigma_c(2455)^0 \overline{p} \pi^+$ [32] and $J/\psi \rightarrow p \overline{p} \pi^0$ [28]. The former is illustrated in Fig. 8; the Dalitz plot for $\overline{B}^0 \rightarrow \Sigma_c(2455)^0 \overline{p} \pi^+$ in particular is strikingly empty close to the baryon-antibaryon threshold.

Baryon formation in the continuum

Enhanced rates near a baryon-antibaryon threshold have also been seen in e^+e^- events with an initial-state radiation (ISR) photon. BABAR has measured the effective form factors for $p \overline{p}$, $\Lambda \overline{\Lambda}$, $\Sigma^0 \overline{\Sigma}^0$, and $\Lambda \overline{\Sigma}^0$ close to threshold [33, 34]; the distributions are shown in Fig. 9. In each case we see a strong enhancement at or close to threshold.

In the charm sector, Belle has recently reported a large structure in $e^+e^- \rightarrow \Lambda_c^+ \overline{\Lambda}_c^- \gamma_{\text{ISR}}$ events, shown in Fig. 10 [35]. They note that the nature of the enhancement is unclear, but that it can be described by an S -wave relativistic Breit-Wigner with mass $4634_{-7-8}^{+8+5} \text{ MeV}/c^2$ and width $92_{-24-21}^{+40+10} \text{ MeV}$. It seems quite plausible that this is one of the many charmonium and charmonium-like states above the $D\overline{D}$ threshold [6]. In particular, it may be the $Y(4660)$ seen previously in $e^+e^- \rightarrow (J/\psi \pi^+ \pi^-) \gamma_{\text{ISR}}$ events [36] with mass $4664 \pm 11 \pm 5 \text{ MeV}/c^2$ and width $48 \pm 15 \pm 3 \text{ MeV}$; the modest discrepancy in parameters be-

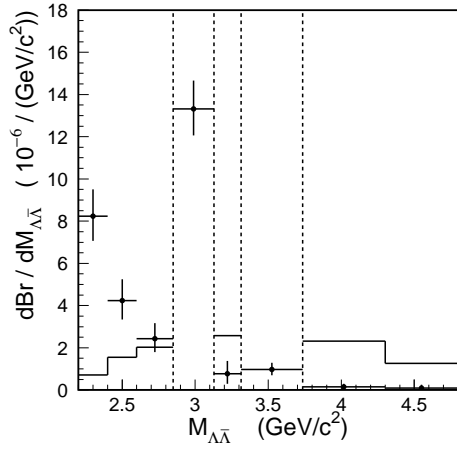
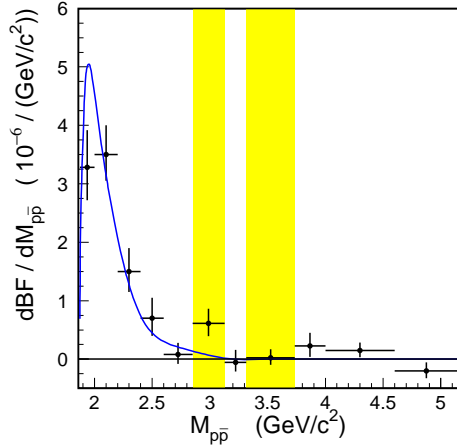
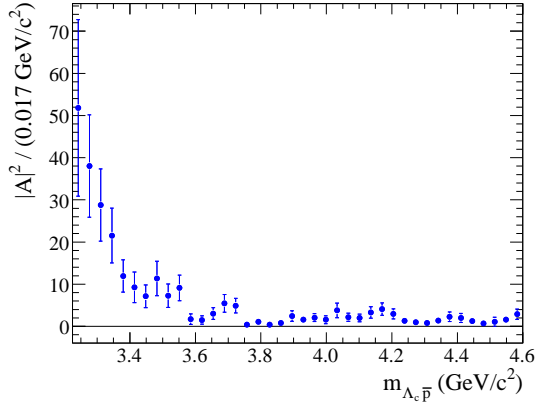


Figure 7: Threshold enhancements. The upper plot (from [7]) shows the projected amplitude squared for $B^- \rightarrow \Lambda_c^+ \bar{p} \pi^-$ decays near threshold after efficiency correction, background subtraction, and correction for the three-body phase space. The middle plot (from [24]) shows the differential branching fraction for $B^+ \rightarrow p \bar{p} \pi^+$; the shaded/yellow bands indicate the two principal charmonium regions and the solid curve is a theoretical prediction [23]. The lower plot (from [26]) shows the differential branching fraction for $B^- \rightarrow \Lambda \bar{\Lambda} K^-$; the dashed lines indicate the two principal charmonium regions, and the solid histogram is a phase-space simulation. The analyses were performed on samples of $383, 449,$ and 657×10^6 $\Upsilon(4S) \rightarrow B\bar{B}$ decays, respectively.

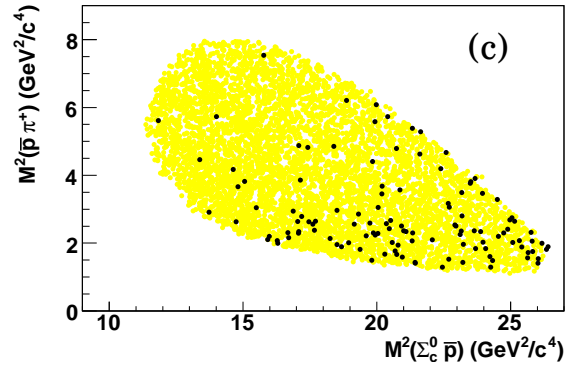
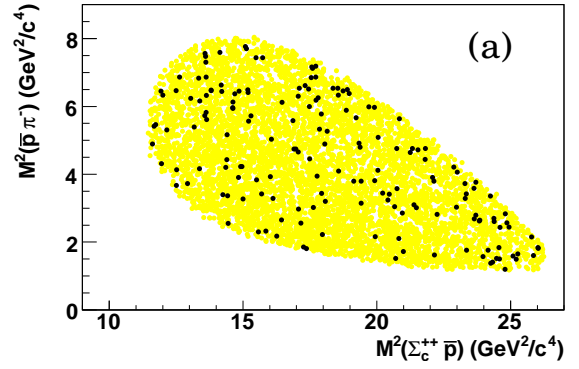


Figure 8: Dalitz plots for $\bar{B}^0 \rightarrow \Sigma_c(2455)^{++} \bar{p} \pi^-$ (upper) and $\bar{B}^0 \rightarrow \Sigma_c(2455)^0 \bar{p} \pi^+$ (lower). The black points represent the data and the yellow/light points are simulated according to three-body phase space. A sample of 388×10^6 $\Upsilon(4S) \rightarrow B\bar{B}$ decays were used. From [32].

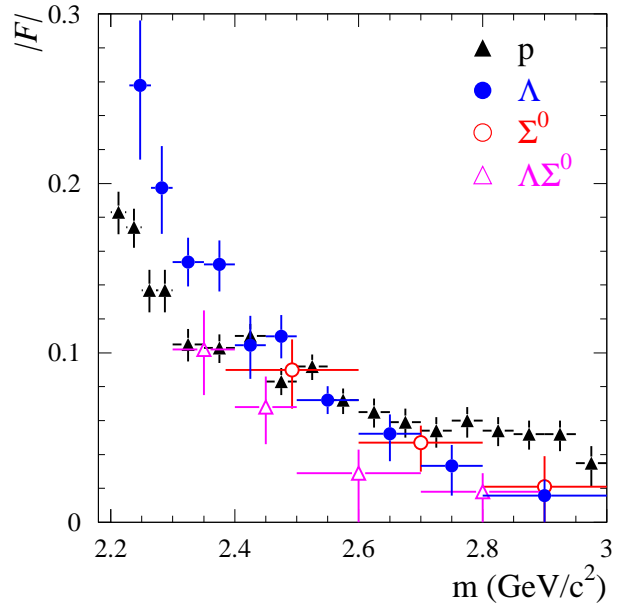


Figure 9: The effective baryon form factors as a function of baryon-antibaryon invariant mass, measured with ISR events in a sample of 230 fb^{-1} of e^+e^- data. From [34].

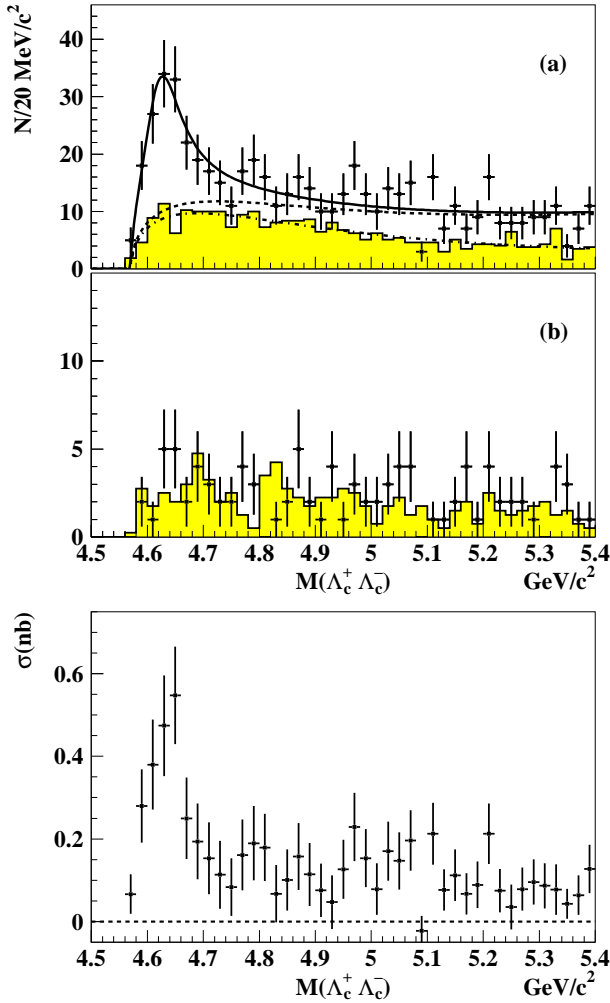


Figure 10: The exclusive process $e^+e^- \rightarrow \Lambda_c^+\bar{\Lambda}_c^-$, measured in $e^+e^- \rightarrow \Lambda_c^+\bar{\Lambda}_c^-\gamma_{\text{ISR}}$ events. Plot (a) shows the $\Lambda_c^+\bar{\Lambda}_c^-$ invariant mass spectrum for events with a \bar{p} tag that lie in the signal region (points) or Λ_c^+ sidebands (shaded histogram). The dot-dashed, dashed, and solid curves represent combinatoric background, a threshold function, and an S -wave relativistic Breit-Wigner function cumulatively. Plot (b) shows equivalent events from the background region. The lower plot shows the corresponding cross-section for $e^+e^- \rightarrow \Lambda_c^+\bar{\Lambda}_c^-$ (after correcting for background, efficiency, and the differential ISR luminosity). Errors shown are statistical only. 695 fb^{-1} of data were used. From [35].

tween the two measurements may be due to differing form factors for the two final states [37].

The kinematic favourability of forming baryon-antibaryon pairs with small relative velocity is certainly not a new discovery or unique to low-energy interactions; it was noted at LEP-I, for example, that correlated $p\bar{p}$, $\Lambda\bar{\Lambda}$, and $\Lambda\bar{p}$ pairs peak at small values of the rapidity difference $|\Delta y|$ [38, 39] and are predominantly produced in the same jet.

This is not universally true, however. In 13.6 fb^{-1} of

e^+e^- data at $\sqrt{s} \sim 10.6 \text{ GeV}$, CLEO studied a sample of continuum events containing both a Λ_c^+ and a $\bar{\Lambda}_c^-$ [40]. (A momentum cut on the Λ_c^+ was used to exclude those baryons produced in B meson decays.) As illustrated in Fig. 11, the charmed baryons in these events are strongly peaked towards $\cos\theta = -1$, i.e. with the baryons in opposite hemispheres. Broadly, there are three possible classes of such events:

1. Events in which the two charm jets fragment independently with one producing a Λ_c^+ and a light antibaryon and the other producing a $\bar{\Lambda}_c^-$ and a light baryon. Baryon number is conserved in each jet, and the invariant mass of and rapidity gap between each baryon-antibaryon pair are small.
2. As (1), except that the fragmentation of the two jets is correlated such that producing a Λ_c^+ on one side makes it more likely that a $\bar{\Lambda}_c^-$ is produced on the other side. Again, baryons are produced in pairs which have invariant mass close to threshold, and baryon number is conserved locally.
3. Events with primary baryon production that contain no baryons besides the Λ_c^+ and $\bar{\Lambda}_c^-$. Baryon number is not conserved in each jet and the baryon-antibaryon pair is far from threshold.

CLEO ruled out the first class as the sole source of the events observed, since the rate was approximately 3.5 times higher than would be expected given independent fragmentation. Qualitatively, they looked for additional protons in the event and did not find signal; this disfavors the second class (since those events have two additional light baryons) but does not exclude it.

BABAR has made a preliminary study of this process with 220 fb^{-1} of data [41]. They see an excess of $\Lambda_c^+\bar{\Lambda}_c^-$ events by a factor of 4, confirming the CLEO observation. In addition, they find that most of the events seen have zero additional identified protons, such that the rate seen is consistent with that expected from material interactions and from misidentification of other charged particles (Fig. 12(a)). Further, when plotting the missing mass distribution of the event (after subtracting the momenta of the Λ_c^+ , $\bar{\Lambda}_c^-$, and any reconstructed tracks), they find that most events have well below $2 \text{ GeV}/c^2$ of missing mass, and are therefore inconsistent with containing a baryon and an antibaryon that are not reconstructed or are misidentified as pions (Fig. 12(b)). While some contribution from classes (1) and (2) is not ruled out, this implies that class (3) is the dominant effect.

Conclusions

There has been a great deal of progress in charmed baryon spectroscopy recently, and the high statistics of Belle and BABAR are still uncovering new states. The use of B meson decays to study resonant states in a fully exclusive environment is a particularly powerful tool; hopefully

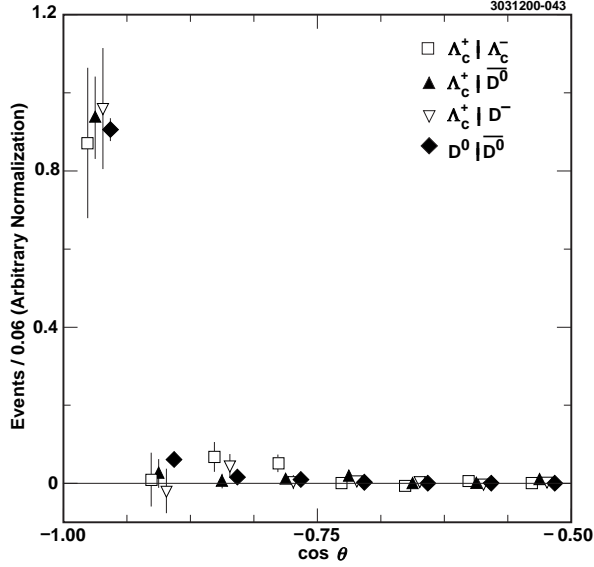


Figure 11: The production angle distribution between various combinations of charmed baryons and charmed mesons. In each case, the charmed particles are approximately back-to-back. From [40].

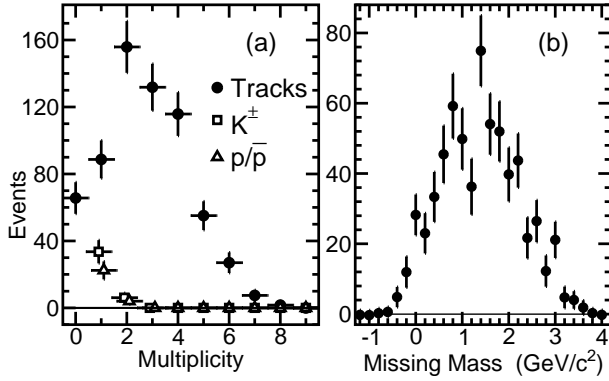


Figure 12: Background-subtracted distributions for events containing $\Lambda_c^+ \Lambda_c^-$: (a) the number of additional tracks, identified K^\pm , and additional identified p/\bar{p} ; and (b) the missing mass, with imaginary masses given negative real values. Most events have no identified K^\pm or p/\bar{p} and the corresponding zero-multiplicity points are off the vertical scale in (a). Preliminary BABAR result—see [41].

it will be extended beyond the $\Sigma_c(2455)$ to measure the quantum numbers of other baryon states.

There are also a number of results finding evidence for threshold enhancements in multi-body baryonic decays. The overall pattern is not clear here, particularly given the absence of an enhancement in some modes. We look forward to further experimental data and to input from phenomenology to help understand these structures.

References

- [1] M. J. Charles, “Charmed Baryons”, presented at CHARM 2009.
- [2] Charge-conjugate processes are implied throughout.
- [3] Unless otherwise stated, the first quoted uncertainty is statistical, the second is systematic, and the third (if present) is due to uncertainty in the $\Lambda_c^+ \rightarrow pK^-\pi^+$ branching fraction.
- [4] BABAR Collaboration, B. Aubert et al., Nucl. Instrum. Meth. **A479** (2002) 1.
- [5] Belle Collaboration, A. Abashian et al., Nucl. Instrum. Meth. **A479** (2002) 117.
- [6] Particle Data Group, C. Amsler et al., Physics Letters **B667** (2008) 1.
- [7] BABAR Collaboration, B. Aubert et al., Phys. Rev. **D78** (2008) 112003.
- [8] Belle Collaboration, N. Gabyshev et al., Phys. Rev. Lett. **97** (2006) 242001.
- [9] Belle Collaboration, R. Mizuk et al., Phys. Rev. Lett. **94** (2005) 122002.
- [10] Belle Collaboration, R. Chistov et al., Phys. Rev. Lett. **97** (2006) 162001.
- [11] BABAR Collaboration, B. Aubert et al., Phys. Rev. **D77** (2008) 012002.
- [12] Belle Collaboration, T. Lesiak et al., Phys. Lett. B **665** (2008) 9.
- [13] BABAR Collaboration, B. Aubert et al., Phys. Rev. **D77** (2008) 031101.
- [14] Belle Collaboration, N. Gabyshev et al., Phys. Rev. Lett. **97** (2006) 202003.
- [15] BABAR Collaboration, B. Aubert et al., Phys. Rev. Lett. **99** (2007) 062001.
- [16] Belle Collaboration, E. Solovieva et al., Phys. Lett. B **672** (2009) 1.
- [17] BABAR Collaboration, B. Aubert et al., Phys. Rev. Lett. **97** (2006) 232001.
- [18] See, e.g., S. Gasiorowicz and J.L. Rosner, Am. J. Phys. **49** (1981) 954.
- [19] ARGUS Collaboration, H. Albrecht et al., Z. Phys. C **56** (1992) 1.
- [20] Belle Collaboration, R. Chistov et al., Phys. Rev. **D74** (2006) 111105.
- [21] P. Zenczykowski, Phys. Rev. D **50** (1994) 402.
- [22] W.S. Hou and A. Soni, Phys. Rev. Lett. **86** (2001) 4247.
- [23] H.Y. Cheng, Int. J. Mod. Phys. A **21** (2006) 4209.
- [24] Belle Collaboration, J.T. Wei et al., Phys. Lett. B **659** (2008) 80.
- [25] Belle Collaboration, M.Z. Wang et al., Phys. Rev. D **76** (2007) 052004.
- [26] Belle Collaboration, Y.W. Chang et al., Phys. Rev. D **79** (2009) 052006.
- [27] BES Collaboration, M. Ablikim et al., Phys. Rev. Lett. **93** (2004) 112002.

- [28] BES Collaboration, J.Z. Bai et al., Phys. Rev. Lett. **91** (2003) 022001.
- [29] D.V. Bugg, Phys. Lett. B **598** (2004) 8.
- [30] B. Kerbikov, A. Stavinsky and V. Fedotov, Phys. Rev. C **69** (2004) 055205.
- [31] G.Y. Chen, H.R. Dong and J.P. Ma, Phys. Rev. D **78** (2008) 054022.
- [32] Belle collaboration, H.O. Kim et al., Phys. Lett. B **669** (2008) 287.
- [33] BABAR Collaboration, B. Aubert et al., Phys. Rev. D **73** (2006) 012005.
- [34] BABAR Collaboration, B. Aubert et al., Phys. Rev. D **76** (2007) 092006.
- [35] Belle Collaboration, G. Pakhlova et al., Phys. Rev. Lett. **101** (2008) 172001.
- [36] Belle Collaboration, X.L. Wang et al., Phys. Rev. Lett. **99** (2007) 142001.
- [37] D.V. Bugg, J. Phys. G **36** (2009) 075002.
- [38] DELPHI Collaboration, P. Abreu et al., Phys. Lett. B **416** (1998) 247.
- [39] OPAL Collaboration, G. Abbiendi et al., Eur. Phys. J. C **13** (2000) 185.
- [40] CLEO Collaboration, A. Bornheim et al., Phys. Rev. D **63** (2001) 112003.
- [41] B.L. Hartfiel, Ph.D. thesis, UCLA, 2005; SLAC-R-823.